J. Fluid Mech. (1966), *vol.* 24, *part* 3, *pp.* 451–479
Printed in Great Britain

Experiments on the onset of thermal convection in horizontal layers of gases

By H. A. THOMPSON† AND H. H. SOGIN‡
Department of Mechanical Engineering, Tulane University,
New Orleans, Louisiana 70118

(Received 11 June 1965)

Precise data are presented on the Rayleigh–Jeffreys instability in air, argon and carbon dioxide at pressures between 0·6 and 6·0 atm in layers of depths $\frac{1}{8}$, $\frac{1}{4}$, and $\frac{3}{4}$ in. A new method yields better resolution and repeatability than the methods employed in the past. Here the gas layer is brought through the state of marginal stability by increasing the pressure while both the temperature and the temperature difference are held constant. The onset of convection is detected by means of a type of heat flow meter ascribed to Prof. L. M. K. Boelter. The equipment and procedure are described and analysed in detail.

The experimentally-determined value of the critical Rayleigh number is 1793, repeatable within a probable deviation of 1% due to random errors. Considering in addition the systematic errors of the instrumentation but not the uncertainties of property values, we place the absolute value within 1793 ± 80. The corresponding theoretical value is 1708.

Finite rates of pressure rise inhibit the development of convection. The results achieved at the least rates of pressure rise are in agreement with steady-state determinations.

The approach employed in this investigation shows great promise as a method for measuring the transport properties of gaseous mixtures or of gases at combined high temperature and high pressure.

1. Introduction

When a shallow horizontal layer of a fluid at rest is heated from below, the fluid at the bottom becomes lighter than the fluid above, the mechanical equilibrium becomes unstable, and 'cellular' motion ensues. Thus we come to the Rayleigh–Jeffreys instability or the Bénard problem. The subject has been reviewed by Ostrach (1957) and authoritatively analysed by Chandrasekhar (1961).

The present work provides experimental data on the instability criterion in three gases, namely air, argon and carbon dioxide, in $\frac{1}{8}$, $\frac{1}{4}$ and $\frac{3}{4}$ in. layers. While we have not yet put our apparatus to its full purpose, we report our findings because they establish that the point of instability possesses a more reproducible nature than has heretofore been expected.

† Assistant professor. ‡ Professor.

Rayleigh (1916) formulated a stability criterion by seeking a steady-state solution of the governing equations of motion at the point of marginal stability. Today that criterion is expressed in terms of the Rayleigh number

$$R = (L^3 g/\kappa\nu)\,\alpha\Delta T. \tag{1.1}$$

Here L is the height of the fluid layer, g is the local acceleration due to gravity, α, κ and ν are fluid properties, namely the volume expansivity, the thermal diffusivity and the kinematic viscosity.† The quantity ΔT is the difference $(T_o - T_u)$ between the temperatures at the lower and upper surfaces. The value of R at the onset of motion is the critical Rayleigh number, denoted by R_{cr}. It depends on the hydrodynamic and the thermal boundary conditions and the temperature distribution at marginal stability, as has been clearly demonstrated by Sparrow, Goldstein & Jonsson (1964). In the case when the top and bottom surfaces are both rigid and highly conducting (fixed temperatures or infinite Biot numbers, in the terminology of Sparrow, Goldstein & Jonsson) and the initial distribution is linear, the theory yields the value 1708. This is the maximum value for any combination of boundary and initial conditions on a fluid of infinite breadth, and it is the value against which our experimental results are to be compared.

Experiments on liquids have yielded remarkable agreement with the theory. R. J. Schmidt & Milverton (1935) found R_{cr} for water at 1770 ± 140. E. Schmidt & Silverston (1959), experimenting with five liquids, found it at 1700 ± 51. Further, beyond the transition, the cellular convection increases the rate of heat transfer, and the Nusselt number becomes dependent on the Rayleigh number.

Experiments on gases have been less systematic. Precise determinations in the same apparatus of R_{cr} for more than one gas have been unavailable. De Graaf & Van der Held (1953), as a by-product of their work on the heat transfer through air layers, placed R_{cr} at 'about 2000'. R. J. Schmidt & Saunders (1938) gave approximately the same value. Chandra (1938) and Dassanayake (Sutton 1950) experimented on air and carbon dioxide, respectively, in essentially the same apparatus. They found qualitative agreement with the theory.

The low experimental resolution in the past investigations on gases may be ascribed primarily to the low heat flux associated with gases, for this limits the effectiveness of the methods successfully employed on liquids. When resistance heaters are used at the bottom surface, the increased electrical current required by a small change in heat flux is difficult to measure. An even more adverse situation exists if the top heat exchanger is employed as a calorimeter: either the upper surface deviates from the ideal isothermal condition or extremely small changes in temperature differences must be measured. The optical methods employed by Schmidt & Saunders and de Graaf & Van der Held for visualizing the onset of motion require measurements beyond transition in order that density differences in the flow field be detectable.

The smoke injection experiments of Chandra and Dassanayake were performed with rapid temperature transients from convection to pure conduction; the

† In this report all the thermal properties have been evaluated at the arithmetic mean temperature $T_a = \frac{1}{2}(T_o + T_u)$. The local value of g is 32·1317 ft./sec^2.

exact nature of the boundary conditions and the temperature distribution at the time of transition were undefined.

In the present work these uncertainties have been avoided by the insertion of extremely sensitive Boelter heat flow meters (Jakob 1957) adjacent to the upper and lower surfaces bounding the gas layer. The instrumentation has been used to determine R_{cr} within a mean error of 1 %.

The procedure most conveniently used with this apparatus is to force the gas layer through the transition by changing the pressure. It may be illustrated by consideration of the following form of the Rayleigh number for an ideal gas at moderate pressures, in which $\mathscr{R}, p, \mu$ and k are the gas constant, the pressure, the dynamic viscosity and the thermal conductivity, respectively.

$$R = \frac{L^3 g c_p \Delta T p^2}{\mu k \mathscr{R}^2 T_a^3}. \tag{1.2}$$

To deduce (1.2) from (1.1), we have employed the relationships $\alpha T_a = 1$, $\mu = \nu\rho$, $k = \kappa c_p \rho$, and

$$p = \rho \mathscr{R} T. \tag{1.3}$$

In our main experiments we fix the temperatures at the two rigid surfaces while the pressure is increased either at a very slow rate or in very small steps. Since the thermal properties in (1.2) are virtually pressure independent, R increases with the square of the pressure. Meanwhile the heat flux q is monitored by means of the very sensitive heat flow meters. Now

$$q = \frac{k\Delta T}{L} f(R), \quad \begin{cases} f(R) = 1 & (R < R_{cr}), \\ f(R) > 1 & (R > R_{cr}). \end{cases} \tag{1.4}$$

Further, $f(R)$ increases monotonically if $R > R_{cr}$. Thus in the conduction region the heat flux through the gas layer is independent of the pressure whereas in the convection region it increases with the pressure.

This type of experiment is depicted schematically in figure 1 for a given gas being pressurized at fixed ΔT and fixed T_a. The heat flux and the Rayleigh number are plotted against the pressure, and the break in the flux curve is associated with R_{cr}.

An alternate method for determining the critical Rayleigh number is to change the temperature difference while holding the pressure constant; this is the method used by all the other investigators.

From the general viewpoint taken by Chandrasekhar (1961, Ch. 1), the onset of motion should occur regardless of the parameter employed to move the Rayleigh number through its critical value.† One of the objectives of the present work has been to check this view. Another objective was to assess the feasibility of employing the transition point for measuring both μ and k in gas mixtures by determining the precision with which R_{cr} can be measured. The idea is to measure the thermal conductivity in the range of pure conduction and to determine the product μk by means of the instability criterion.

† Another very attractive way is to reduce T_a at constant p and constant ΔT. For, as the transport process changes from the conductive to the convective mode, the heat flux passes through a minimum!

In §2 the apparatus is described in considerable detail. The estimate of the relative error in R is discussed in §3. The time delay of the meter response is also treated. The experimental results are presented and discussed in §4. An interesting finding is that R_{cr} tends toward significantly higher values as the rate of pressure rise increases.

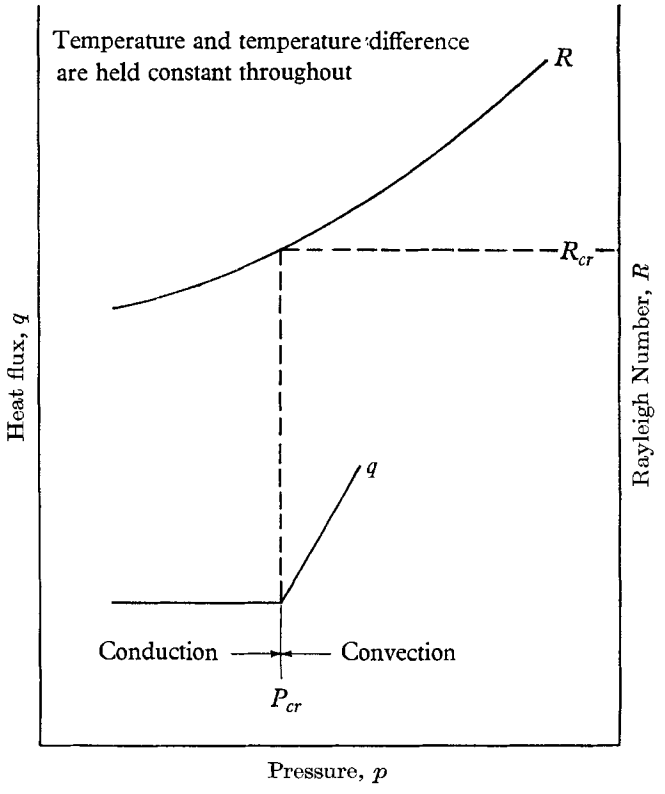

FIGURE 1. Graphical representation of experimental procedure.

Owing to the broad selection of the specific heat ratio and the precision of the experimentation, the results show without doubt that the Rayleigh number is properly based on the specific heat at constant pressure. This was not always clear during the course of the investigation, for two reasons. First that Chandrasekhar specifies that the specific heat at constant volume be used for a gas and second that a set of unfortunate circumstances surrounding the experiment, later traced to a small sub-atmospheric leak into the apparatus, yielded results on air and argon that were very well correlated with the specific heat at constant volume (Thompson 1964). After the experimental difficulty had been rectified, the error in Chandrasekhar's analysis was uncovered. The correct perturbation analysis and the effect of finite dilatation on the stability problem are presented in an appendix.

The conclusions are itemized in §5.

2. Description of the experimental apparatus

A cross-sectional diagram of the experimental apparatus is shown in figure 2. The gas layer is bounded above and below by essentially identical units. Each unit consists of three components: a copper cover plate A, a heat flow meter package B, and a copper heat exchanger C, all bonded together in thermal contact.

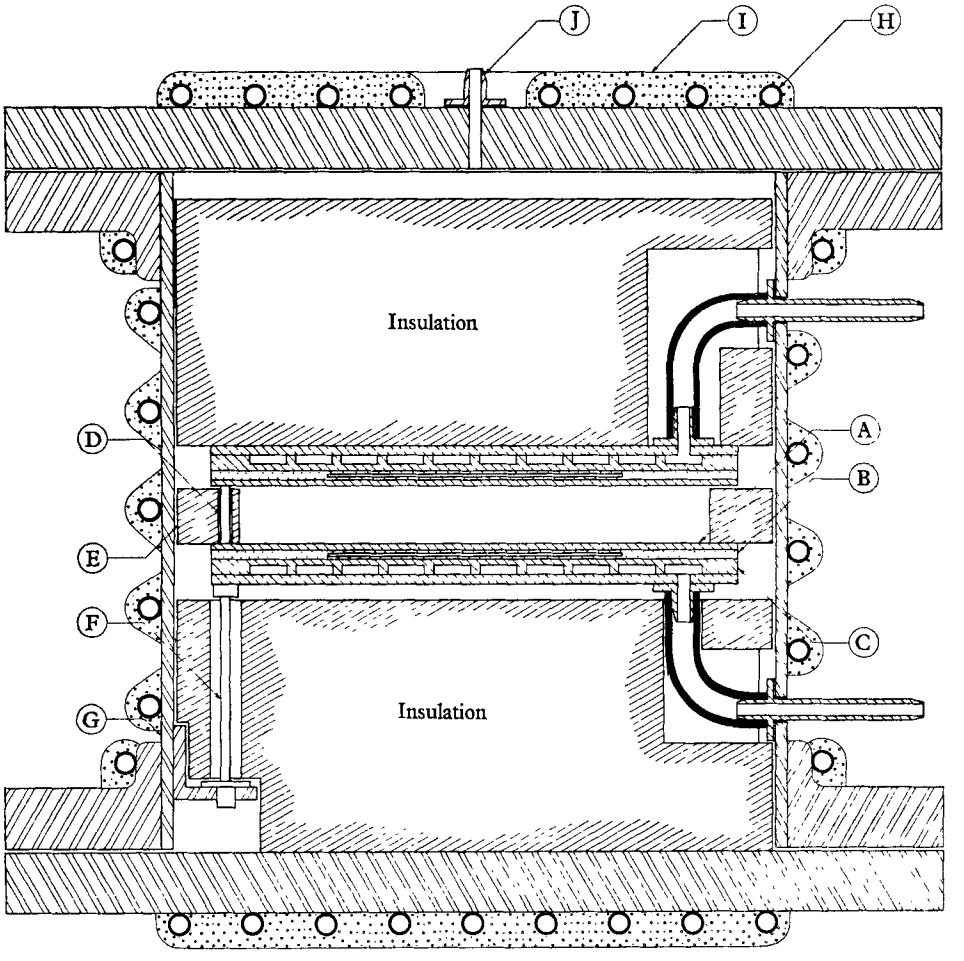

FIGURE 2. Cross-sectional elevation of the apparatus.

The heat exchangers C are of the single cross-flow type. They were formed from $\frac{5}{8}$ in. electrolytic copper plates $10\frac{3}{4}$ in. in diameter. The flow passages were milled, and closure plates were attached. Water from Colora Ultra-Thermostats, Type HT 17, is circulated through the exchangers at a rate of approximately 1.8 gal./min. This flow rate yields a temperature change in the cicrulating water computed to be 0·018 °F at maximum heat load. The lower exchanger is built with an upwardly sloped flow passage and vented at the high point to allow for removal of any oxygen coming out of solution from the circulating water.

Each heat flow meter package B consists of three glass-bonded mica sheets $10\frac{3}{4}$ in. in diameter by $\frac{1}{16}$ in. thick, bonded in a sandwich-like arrangement. A 6 in. square is removed from the centre of the middle sheet, and twelve Boelter heat flow meters are mounted in this square. Each meter is formed from approximately 600 turns of 0·005 in. diameter constantan wire wrapped along the central $5\frac{1}{2}$ in. of a glass-bonded mica strip 6 in. long by $\frac{1}{2}$ in. wide and $\frac{1}{16}$ in. thick. The sensitivity of each meter is approximately 0·13 mV h ft.^{2}/B.Th.U., and the response is linear. Leads from the meters in the bottom package are brought out individually so that the output of any single meter may be read or any number of the twelve may be connected in series.

The copper cover plates A are $10\frac{3}{4}$ in. in diameter by $\frac{1}{8}$ in. thick. The exposed surfaces of these plates were lapped and polished to within 0·0001 in. of flatness. These plates minimize radiative heat transfer across the gas layer, aid in maintaining the height of the layer and smooth any departures from the ideal isothermal condition of the bounding surfaces that might have been introduced by the presence of the constantan wires in the meters.

The height of the fluid layer, or the gap size, is maintained by a set of three $\frac{1}{4}$ in. diameter poly(methyl methacrylate) spacers D placed around the edge of the lower surface at 120° intervals. Each set of spacers is made so that the maximum difference in length is no more than 0·0001 in. Actual heights are determined by correcting the spacer lengths both for the compressive shortening due to the load impressed by the upper surface and for thermal expansion. Lateral support for the spacer rods during assembly is provided by an annular ring of heavy-duty styrofoam insulation E which serves the dual purpose of reducing radial heat transfer into the gap. To provide access to the layer for the gas admitted during a run, the thickness of the annular ring is at least 0·020 in. less than the height of the spacers D.

The lower heat exchanger is supported by three steel pedestals F attached to the pressure vessel. The pressure vessel G is formed from 12 in., schedule 40 pipe, with flanges welded at the ends; the vessel is closed by means of blind flanges. To minimize disturbances of the system, the pressure vessel is placed on a 1700 lb. concrete block mounted on four vibration absorbers. This arrangement was found to virtually eliminate the effect of floor vibrations above 2 c/s. As an additional precaution rubber hose is used in making circulating water connexions to the pressure vessel. The bottom surface may be levelled to within $\pm$ 0·0005 in./ft. of horizontal distance by means of levelling screws on the bottom flange of the vessel. For levelling this surface after bolting the blind flange and for checking the level during operation, two flat bars are placed on the outside of the vessel. These bars may be adjusted parallel to the surface and locked in place. Control of the temperature of the walls bounding the gas layer is provided by coils of copper tubing H attached to the pipe and blind flanges with heat-transfer cement I. Water from a third Colora thermostat is circulated through these coils. Finally, the entire vessel is covered with a 1 in. thick layer of Thurane FR insulation.

Gas enters the pressure vessel through the nozzle J. In the vessel it moves radially along the underside of the blind flange to the vertical wall. It then

moves downwards along the wall to the annular plenum chamber surrounding the heat exchangers. From this chamber the fluid moves into the gas layer. The velocity is sufficiently low for the fresh inlet gas to be brought into thermal equilibrium with the interior of the pressure vessel and 'conditioned' prior to entering the layer by contact with the heat exchanger.

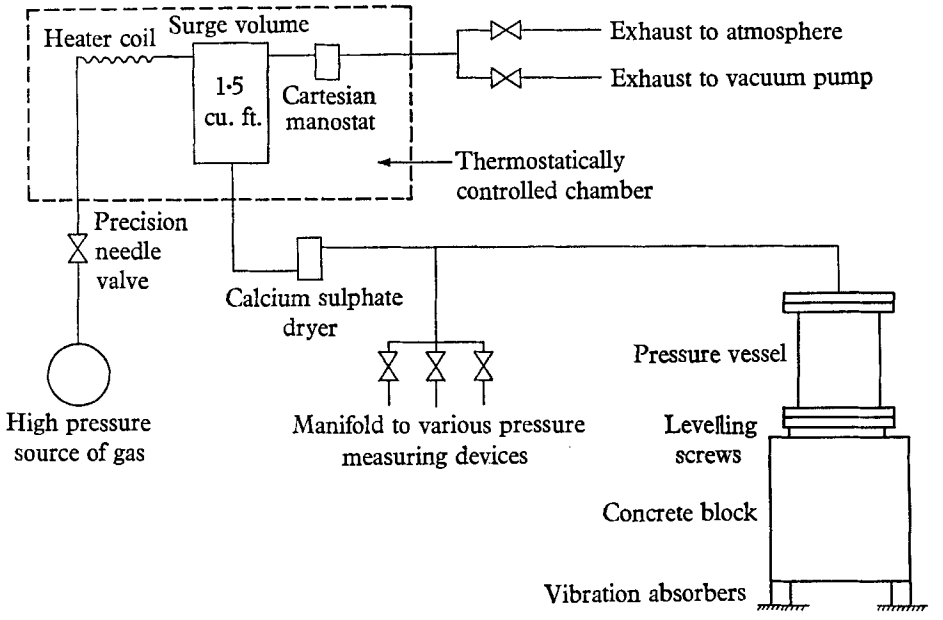

FIGURE 3. Diagram of pressure control system.

The gas inlet nozzle J is connected to the surge tank in the pressure control system. A schematic flow diagram of this system is shown in figure 3. A precision needle valve is located downstream of a high-pressure source of the working gas. Gas from the valve passes through a coil-type heat exchanger into a 1·5 cu.ft. surge volume, then through a Cartesian manostat. The effluent from the manostat exhausts, depending on the pressure level, either to the atmosphere or to a vacuum pump. The coil, surge volume and manostat are maintained isothermal in an enclosure at 125 °F. Gas from the surge tank in the pressure control system reaches the pressure vessel by flowing through a calcium sulphate dryer rated for a dew point of -100 °F. This scheme was selected because it provides pressure control in the gas layer and is effective even at zero flow. Studies of the system with a Betz manometer showed that the standard deviation of the measured pressures was 0·007% of the set value. By blocking the valves downstream from the manostat and adjusting the metering valve, controlled rates of pressure rise as low as 0·20 mmHg/min can be obtained.

Where transition is induced by changing pressure, both mean temperature and temperature difference are held constant. Essentially this is accomplished by controlling the temperature of the top surface at a fixed value and regulating the bottom to keep the temperature difference between the two surfaces con-

stant. A diagram of the control system used in this mode of operation is shown in figure 4.

The temperature of the top surface is held fixed by means of the corresponding Colora thermostat. The control element of these thermostats is a contact thermometer, and the action is on–off. Before each run this thermostat may be

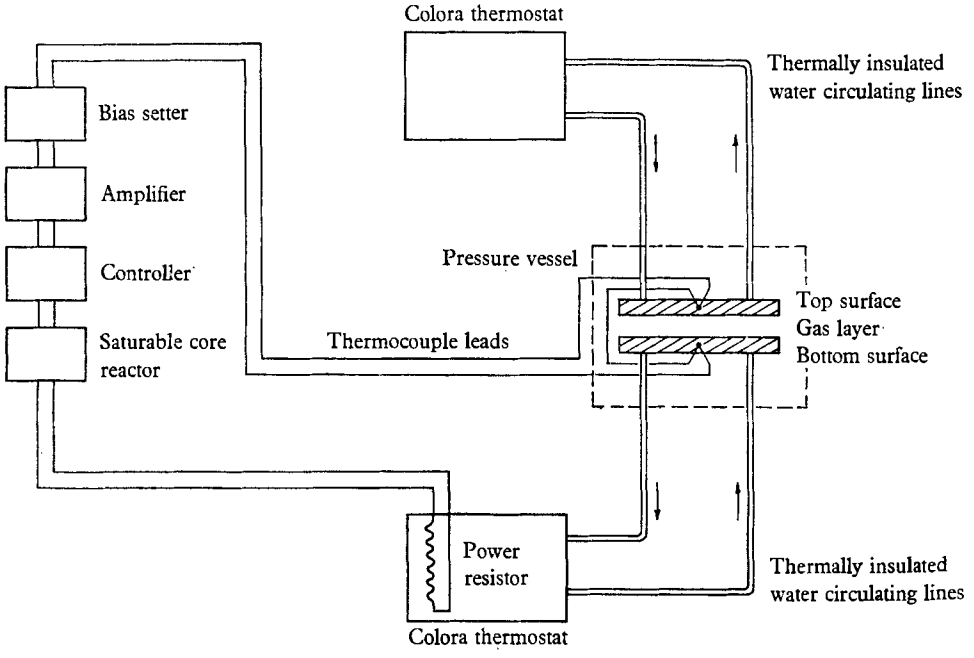

FIGURE 4. Diagram of temperature and temperature-difference control systems.

adjusted for optimum control; that is, it can be adjusted until the top surface temperature, measured by means of a Leeds & Northrup K-3 potentiometer at its most sensitive setting, shows no detectable variation with the cycling of the thermostat control system. This cycling is picked up by the heat flow meters in the top surface, however, and appears as a sinusoidal variation amounting to as much as $\pm 8\,\%$ of the output.

The system employed to control the temperature difference consists of a Leeds & Northrup bias setter, d.c. amplifier, 3-action controller, and saturable core reactor. A pair of thermocouples, one in the top and one in the bottom surface bounding the gas layer, are connected so that their differential output is opposed by a voltage from the bias setter which is equivalent to the desired temperature difference. Deviations of the temperature difference from the set e.m.f. are put through the d.c. amplifier and then into the controller. The controller drives the saturable core reactor connected across a power resistor located in the circulating water bath of the bottom thermostat. (The built-in control system of this thermostat had previously been intentionally rendered inoperative.) Long-term variations in the temperature difference during any run are less than 0·03 °F. After proper adjustment of the controller, the influence of control action on the lower heat flow meter is less than $0{\cdot}5\,\%$ of the output

at a temperature difference of 18 °F and not more than 1 % at the lower heat flux levels encountered in the present research.

The thermocouples were prepared from 0·010 in. diameter copper and constantan wire of premium grade. The wire was calibrated against a Leeds & Northrup 8163-C platinum resistance thermometer in conjunction with a G-2 Mueller bridge. The standard deviation of the sample thermocouples from a single curve of e.m.f. versus temperature was 1.14 μV. Indications of the upper and lower surface temperatures were obtained from three thermocouples bonded between the cover plate and the heat flow meter package of each surface. Checks during operation showed a maximum spread in the output of these thermocouples of 5 μV. This spread reflects not only differences between individual thermocouples but installation differences as well.

Absolute pressures under 800 mm mercury are measured with a Haas Type A-1 barometer. Between 800 mm mercury and two atmospheres absolute, gauge pressure is measured with the Haas barometer operated as a manometer. In this range, changes in atmospheric pressure are detected with a Wallace & Tiernan altitude gauge which has been calibrated against the barometer. Above two atmospheres, gauge pressures are measured with a Model 217 Teledyne pressure transducer manufactured by the Taber Instrument Corporation. This transducer is calibrated against an Ashcroft dead weight tester.

Direct measurements of the purity of the working gas are not made at present. In investigations with air layers, the humidity level of air trapped in the pressure vessel during assembly is reduced to a negligible level by repeated pressurization and evacuation of the vessel through the dryer (figure 3). This procedure is repeated each time the vessel is opened to the atmosphere. When gases other than air are used, repeated dilution of the pressure vessel contents is employed to the point where calculations show the molar concentration of contaminants is less than 0·2 %. The compressed air source is utility air supplied to the laboratory. It passes through a combined strainer and separator before entering the pressure control system. The argon used in these investigations is rated at a purity of 99·995 %, and the purity of the carbon dioxide is in excess of 99·0 %.

An experiment is begun by bringing the system to equilibrium in the conduction region at a point well below transition. The pressure rise is initiated, and a record of pressure and time is kept by reading the pressure at intervals ranging from 1 to 10 min, depending on the rate of pressure rise. These pressure readings are synchronized with the chart speed of a two-channel Honeywell Electronik strip-chart recorder to which upper and lower heat flow meters are connected. As examples, two sections of recorder chart paper taken from entirely separate runs are reproduced in figure 5. In both charts the left-hand (lower-valued) trace is a direct record of the output from heat flow meter elements in the upper surface. The right-hand trace in chart A is a direct record of the output from heat flow meters in the lower surface. The transition is indicated in both meter records on this chart and is the point at which the meter output begins to increase with time. In order to define the location of this point more precisely the output of a meter in the lower surface was opposed by a bucking voltage roughly equivalent in value. The difference between these two voltages was

then amplified by a factor of 200, and it is this record which is shown in chart B of figure 5. Most of the data presented here were obtained using the technique associated with chart A; however, the considerable improvement in the isolation of the location of the transition point as indicated by chart B has been incorporated into our procedure.

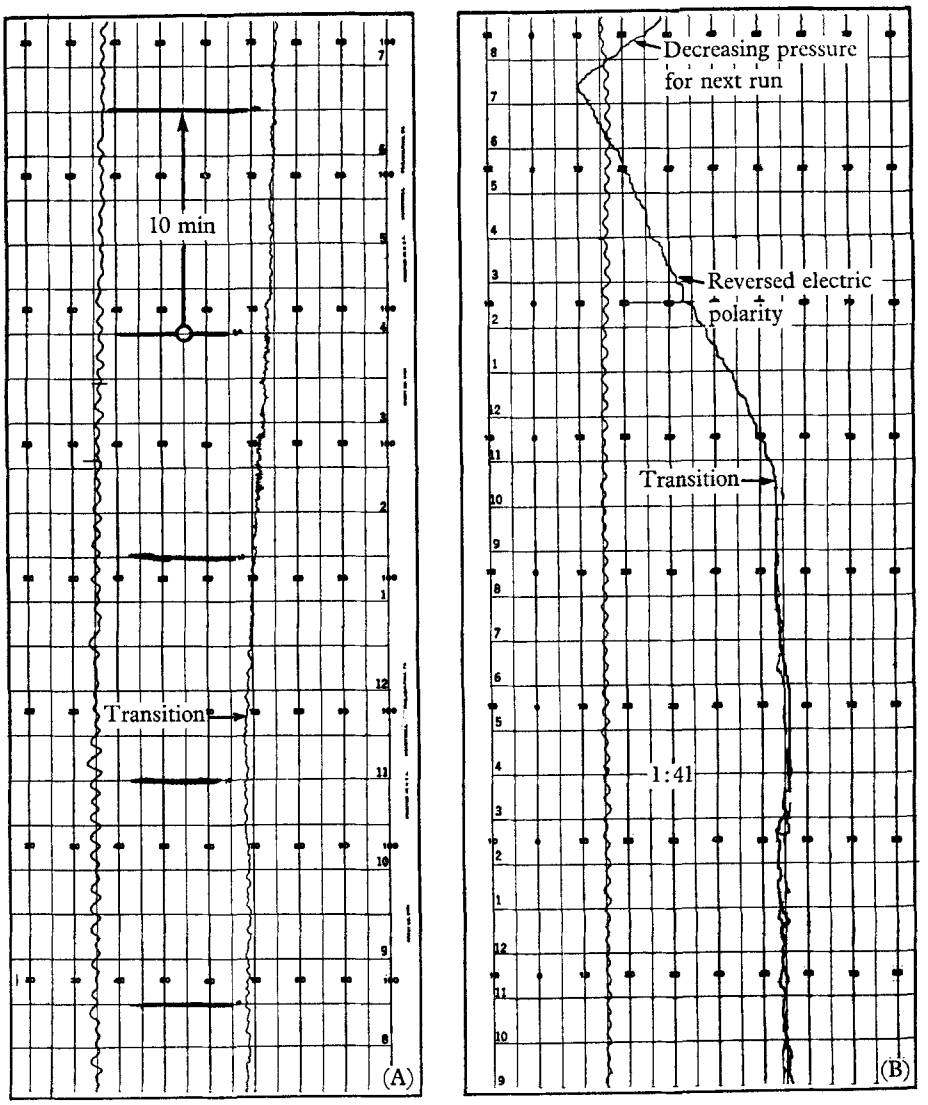

FIGURE 5. Typical records of transition. (A) Air, $\frac{3}{4}$ in. gap, ΔT = 17.64 °F, T_a = 581·2 °R, 1·4 mmHg/min, p_{cr} = 481·6 mmHg; (B) carbon dioxide, $\frac{1}{4}$ in. gap, ΔT = 17·23 °F, T_a = 576·1 °R, 10 mmHg/min, p_{cr} = 24·89 p.s.i.a.

3. Analysis of the experimental errors

Where the physical properties of the fluid layer and the local gravitational acceleration are constant and free of error the relative error in the Rayleigh number may be approximated by

$$\left|\frac{dR}{R}\right| = 3\left|\frac{dL}{L}\right| + 2\left|\frac{dp}{p}\right| + \left|\frac{d(\Delta T)}{\Delta T}\right| + 4\left|\frac{dT}{T}\right|. \tag{3.1}$$

Layer heights are controlled within 0·0001 in. and the contribution of this uncertainty to the relative error varies between 0·72 and 0·12 % as the layer height changes from $\frac{1}{8}$ to $\frac{3}{4}$ in.

Uncertainty in the temperature and temperature-difference measurements arises through uncertainties in thermocouple calibration, differences in individual thermocouples, precision of thermocouple placement and errors in voltage measurements. That is, in equation form,

$$dT \simeq dT_c + dT_i + dT_l + dT_v, \tag{3.2}$$

and

$$d(\Delta T) \simeq d(\Delta T)_c + d(\Delta T)_i + d(\Delta T)_l + d(\Delta T)_v, \tag{3.3}$$

where the subscripts denote, sequentially, calibration errors, differences in individual thermocouples, errors of location and errors in voltage measurements.

With our equipment the maximum error in any single calibration measurement is of the order of 0·01 °K. Within 99 % confidence level, the error present in measurements of mean temperature using two randomly selected thermocouples does not exceed three times the standard deviation of the indvidiual thermocouples divided by the square root of two; accordingly,

$$dT_c + dT_i \leqslant 2{\cdot}33\,\mu\text{V} = 0{\cdot}055\,^\circ\text{K}. \tag{3.4}$$

For the same confidence level, the maximum error in temperature difference measurements with two randomly selected thermocouples is twice the maximum error in the mean temperature measurement,

$$d(\Delta T)_c + d(\Delta T)_i \leqslant 0{\cdot}110\,^\circ\text{K}. \tag{3.5}$$

In (3.1), T and ΔT refer to the mean temperature and temperature difference across the gas layer; however, the thermocouples that measure these variables are between the cover plate and the heat flow meter instead of the interface bounding the gas layer. This introduces systematic errors that depend upon the heat flux level. The maximum value of steady state, conductive heat flux encountered in this investigation was 27·6 B.Th.U./h ft.^{2}. At this level the temperature change across either copper cover plate is of the order of 0·0007 °K. The cover plate is bonded to the heat flow meter package with epoxy cement and by far the most serious consideration connected with the placement of the thermocouples is the thickness of epoxy between the cover plate and the thermocouple junction. From the construction details this thickness can be anywhere between zero and 0·009 in. Assuming an epoxy thermal conductivity of 0·1 B.Th.U./h ft. °F, the estimated temperature change across the maximum thickness of epoxy is 0·110 °K. Considering the mean temperature alone, we find the worst

case is a zero epoxy thickness for one surface, so that the thermocouple junction for that surface is against the cover plate, while the junction in the other surface is separated from the cover plate by the maximum thickness of epoxy and contacts the heat flow meter package. However, for the overall problem the worst case is that both epoxy thicknesses are at the maximum; this is to say that upper and lower junctions would be in contact with the heat flow meter packages. Since these cases are mutually exclusive only the worst case from the standpoint of the overall problem is considered; hence

$$dT_i = 0 \tag{3.6}$$

while

$$d(\Delta T)_l = 0{\cdot}220\,^{\circ}\mathrm{K}. \tag{3.7}$$

Limits of error on temperature readings with the K-3 potentiometer are 0·015 % plus 0·5 μV. For a mean temperature of 325 °K the maximum error in a single temperature measurement is approximately 0·02 °K; accordingly,

$$dT_v \simeq 0{\cdot}02\,^{\circ}\mathrm{K}, \tag{3.8}$$

and

$$d(\Delta T)_v \simeq 0{\cdot}04\,^{\circ}\mathrm{K}. \tag{3.9}$$

At a mean temperature of 325 °K the sum of the contributions of the several uncertainties in the absolute temperature measurements to the relative error in the Rayleigh number is 0·09 %. Because the temperature difference ΔT is much less than the absolute temperature, its total relative error is much larger than that of T; thus, at a difference of 10 °K the total relative error in ΔT is 3·7 %.

The greatest relative error in our pressure determinations occurs at the lowest pressure levels where the absolute value of the pressure measurement is accurate to better than 1·0 mm Hg. At a total pressure of 475 mm Hg the contribution of this error to the uncertainty in the Rayleigh number is 0·4 %.

The sum of these contributions shows the maximum possible error in the experimentally determined Rayleigh number must be less than 4·3 %. This figure is a measure of the reproducibility of the absolute value of the Rayleigh number and includes both random and systematic errors. To determine the repeatability limit the systematic errors peculiar to our apparatus are eliminated and the uncertainty in the Rayleigh number, which is due solely to random errors, is 1·2%. This number indicates the minimum resolving power of the equipment; that is, the capacity to repeat a particular value of the Rayleigh number.

Data on the physical properties of the gases were taken from *N.B.S. Circular* 564 by Hilsenrath *et al.* (1955). Since they report their correlations showing deviations of 1 and 2 %, we must conclude that the uncertainty in the determination of the absolute value of R_{cr} is somewhat greater than 4·3 %. This estimate is, however, based on the most adverse combination of coincidental errors. For the larger gap sizes, the uncertainty in the apparatus is considerably less.

The use of the 1·0 mm Hg uncertainty in the pressure measurement implies not only an ability to measure pressure but also to synchronize this measurement with the onset of convection. This consideration raises the question of the transient response of the heat flow meter and the copper cover plate to changes occurring in the gas layer.

This question is depicted in figure 6, where the e.m.f. of a heat flow meter is sketched as a function of pressure (or time). The origin $O(p_{cr}, E_c)$ represents the point of transition. Curve A is a hypothetical response that would be seen if the convection would begin suddenly and there were no lag in the instrumentation. The response that we actually see on the chart is depicted by curve B, except

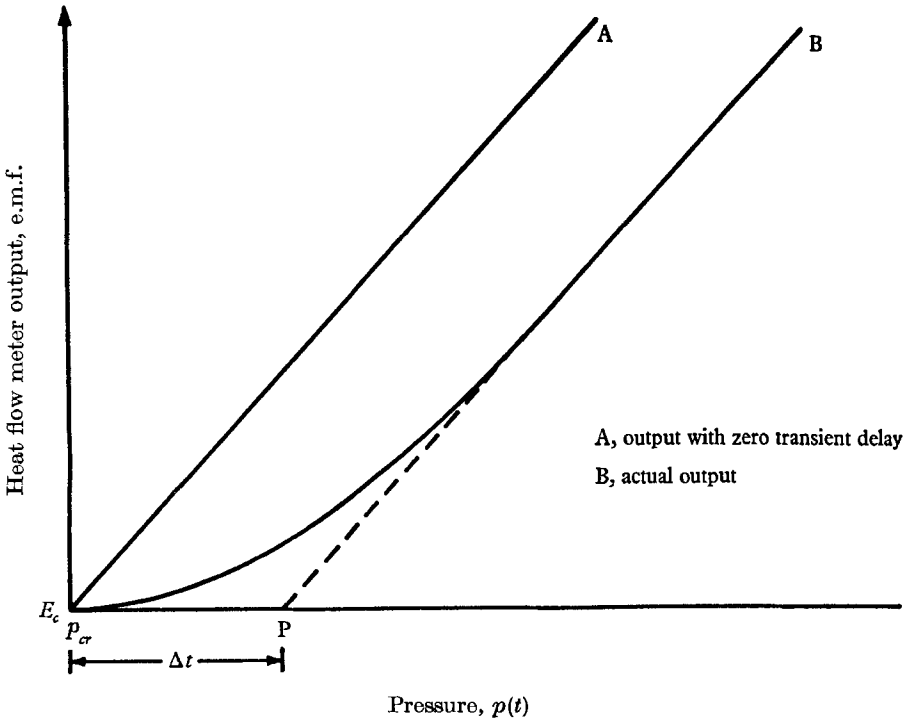

FIGURE 6. Schematic response of the heat flow meters.

that the lower part, exaggerated here for clarity, is in reality very difficult to resolve. In reducing some of the recorder data we extrapolated along the dotted line down to the axis of abscissae to find the apparent critical pressure at P. Thus OP corresponds to a time delay Δt, and the product of Δt and the rate of pressure rise should be deducted to determine the true critical pressure. The time delay introduces an uncertainty, and it is obviously important that we have an estimate of its value.

An analysis of the meter response is outlined in Appendix A. It shows that Δt is approximately 1·5 min, and is independent of the type of gas, the depth of the layer and the rate of pressure rise. This calculated delay is in qualitative agreement with results from preliminary experiments on the heat flow meter packages. They were inserted in a guarded hot plate apparatus, brought to steady state and subjected to a sudden change of source current. The measured time delay was about 0·5 min. Clearly, in testing at very low rates of pressure rise, particularly at high pressures, a time-lag of 1·5 min can be readily accounted for, as has been done in §4.

Since relative changes of the heat flux adequately indicate the onset of motion, extensive meter calibrations, establishing a relation between the heat flux and the meter output, are not required. When gas properties are known the value of the critical Rayleigh number may be established, without absolute heat flux measurements. Without these calibrations or a flow visualization technique it is necessary to assume that simple molecular conduction occurs when the meter e.m.f. is independent of the pressure. The experiments described below indicate that this assumption is sound.

4. Results and discussion

Typical data obtained by increasing the pressure are shown in figure 7, in which the e.m.f. ratio E/E_c determined from the output of three heat flow meters is plotted against pressure. Subscript c signifies the output in the conduction region. Runs at two temperature differences are shown. Initially, as the pressure increases, E/E_c is independent of pressure and stays approximately one. The variation about unity is present even at constant pressures far below transition. Such a variation must be expected from hunting action of the control system. At a particular pressure, E/E_c departs from unity and becomes pressure dependent. That pressure is taken as the transition value in computing the critical Rayleigh number.

Several features of the apparatus and the experimental procedure were investigated to determine their effect on the value of the critical Rayleigh number. The influences of the rate of pressure rise, mass increase within the layer, Biot number, mechanical perturbations and wall temperature were examined experimentally. The results of these investigations are summarized in the following discussion.

The rate of pressure rise may influence our observation of the critical Rayleigh number through several diverse mechanisms. As already indicated, if the delay of the heat flow meter response to changes in the gas layer is long by comparison with the time required to raise the pressure, the critical Rayleigh number will appear dependent on the rate of pressure rise. Furthermore, increasing the pressure of the gas layer at both constant mean temperature and constant temperature difference induces a non-zero velocity owing to the movement of the make-up fluid. This contradicts the assumption of an initially stagnant layer in the theoretical development. Sparrow *et al.* (1964) have shown that the value of the critical Rayleigh number decreases as the initial temperature distribution across the layer deviates from the linear one associated with pure conduction. Augmentation of the mass within the layer may influence the critical Rayleigh number not only through its effect on the hydrodynamic initial condition but also through changes of the initial temperature distribution. Since the ideal stagnant gas layer can only be *approached* experimentally, the pertinent question is whether the motion of the make-up gas or the method of its introduction causes a significant variation in the results.

A plot of experimentally determined critical Rayleigh number versus rate of pressure rise is presented in figure 8. These points were determined by the method of extrapolation outlined near the end of §3. The data cover a range

of rates from 36 mmHg/min down to the zero value of steady state;† the layer heights of $\frac{1}{8}$, $\frac{1}{4}$, and $\frac{3}{4}$ in. are included. Below about 2 mmHg/min the effects of the rate of pressure rise cannot be resolved in this diagram, but on the average the points indicate a persistent influence of the filling. Subsequent conclusions of the evaluation of R_{cr} are based on data obtained at the low rates as well as at steady state.

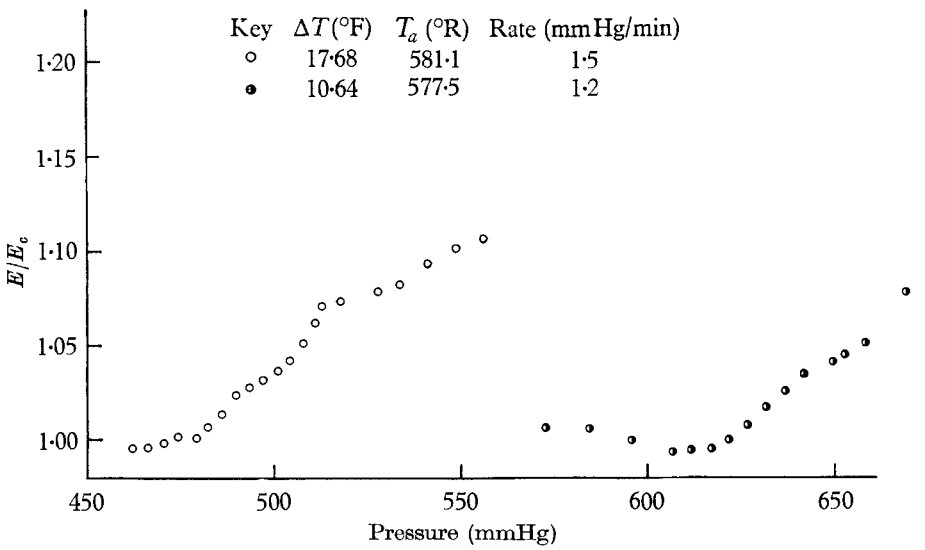

FIGURE 7. Effect of pressure on heat transfer across a horizontal air layer 0·749 in. thick, with temperature difference as parameter.

The solid curve in figure 8 has been faired through the carbon dioxide points. The dotted curve shows the trend after adjusting for the delay of 1·5 min in the instrumentation, as mentioned in §3. The curves indicate that the variation of the critical Rayleigh number at high rates of pressure rise cannot be explained solely in terms of the transient response of the measuring system. The interesting aspect of this is that the higher rates of pressure rise seem to impede the development of the convective motion.

Pellew & Southwell (1940) indicated that if the vertical wall conducts heat horizontally it would be a serious deterrent to successfully approximating an infinite layer. We investigated the influence of wall temperature in a sequence of runs in which the metal wall was maintained first at the temperature of the top surface and then at the temperature of the bottom surface. These severe differences were moderated by the presence of the styrofoam annular insulation. Two of these runs are presented in figure 9. Regardless of whether the metal wall is at the top or bottom surface temperature, transition occurs at the same pressure. We conclude that within the range of our experiments the lateral heat conduction is without influence on the observed point of transition. There

† That is, a sequence of many tests in which the pressure of a single configuration is changed in small steps up and down the scale and all the measurable quantities are given ample time to cycle within the limits of control; the critical point is determined as before.

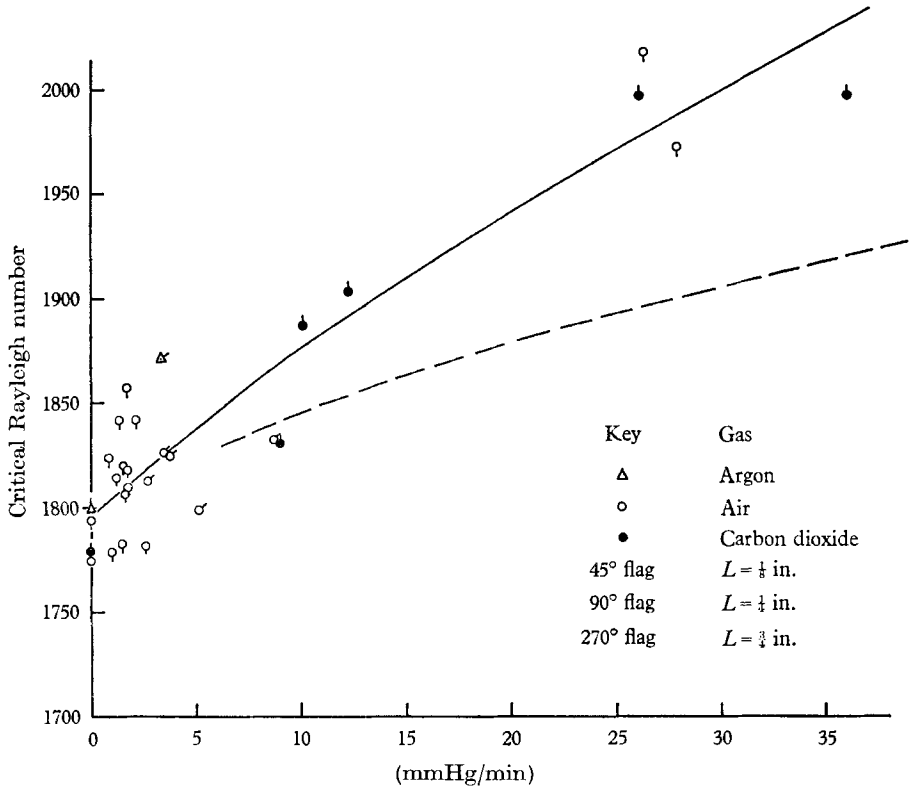

FIGURE 8. Influence of rate of pressure rise on the critical Rayleigh number.

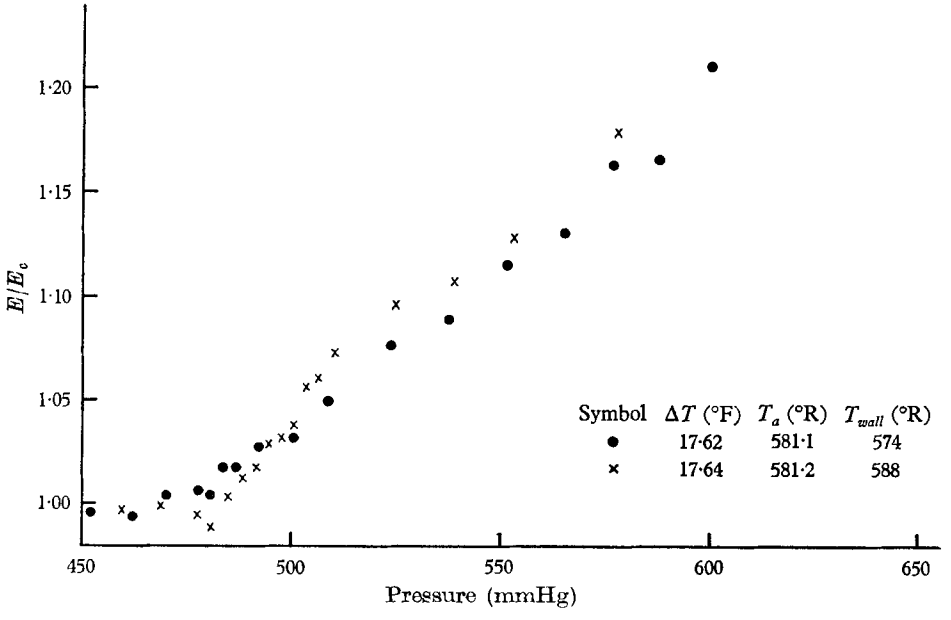

FIGURE 9. Influence of wall temperature.

is a peculiar saltant behaviour (not shown in the coarse structure of figure 9) in the output of the bottom heat flow meter when the metal wall is closed to the bottom plate temperature. This behaviour starts shortly after transition and occurs intermittently for 10 or 15 min thereafter.

Rather severe mechanical disturbances had no detectable effect. The system was brought to equilibrium some 40 mmHg below transition. The pressure was *abruptly* increased to 1 % below the transition value and controlled at that point. There was no detectable change in heat flux. The concrete block supporting the pressure vessel was then struck repeatedly with a hammer. When hammering produced no effect the pressure vessel was deflected approximately $\frac{1}{2}$ in. so that it rocked on its vibration absorbers and, again, there was no detectable change in the heat flux. Increasing the pressure 10 mmHg to about 1 % above the critical value tripped the transition. Moreover, the flux remained fixed at its higher value until the pressure was increased again.

Below transition the heat flow meter output is independent not only of pressure but also the rate of pressure rise. This indicates that, at Rayleigh numbers less than critical, the magnitude of the motion induced either by the injection into the layer, or by the impressed mechanical disturbances, is not sufficient to cause a detectable departure from a purely conductive mode of heat transfer.

It may be argued that the heat flow meters are not sufficiently sensitive to pick up the effects of the disturbances put upon the apparatus. However, the significant point is that the magnitude of the disturbances associated with the onset of motion are much greater than those impressed externally.

Past studies of the point of marginal stability employed the temperature difference to vary the Rayleigh number. To establish whether the pressure variable introduces any significant differences, a series of runs was performed in which the temperature difference was varied.

Modifications to the equipment were minor. The sensing element for the bottom temperature control was changed by substituting a thermocouple maintained at the ice point for the reference thermocouple in the top surface. The voltage source was now set to an output equivalent to the desired bottom temperature instead of temperature difference.

The procedure for these runs was to bring the apparatus to equilibrium at uniform pressure while the temperature difference was well below critical. The temperature difference was increased by reducing the top surface temperature while maintaining the bottom surface temperature constant. The top thermostat was adjusted not for optimum control but for a very slow decline of temperature when the current to its heaters was shut off. As it cooled, the top surface temperature was measured at 5 min intervals. Indication of the heat flux, E, was obtained by recording the sum of the outputs from three of the elements in the bottom heat flow meter. Data from a representative run in this series are shown in figure 10. This figure is a plot of E and E_c versus temperature difference. Determination of E_c required calibration of the heat flow meters. This was done by bringing the apparatus to steady state at various temperature differences throughout the range of the runs, while the pressure at each difference was well below transition. The plot of temperature difference versus meter output, E_c,

in the conduction region was thereby constructed. This curve shows that, in the range of mean temperatures investigated, E_c was a linear function of the temperature difference. These data on E and E_c are combined in figure 11 to provide a plot of E/E_c versus temperature difference.

Although noise levels in the conduction region are increased somewhat, the data in figure 11 show the same characteristic increase in E/E_c beyond

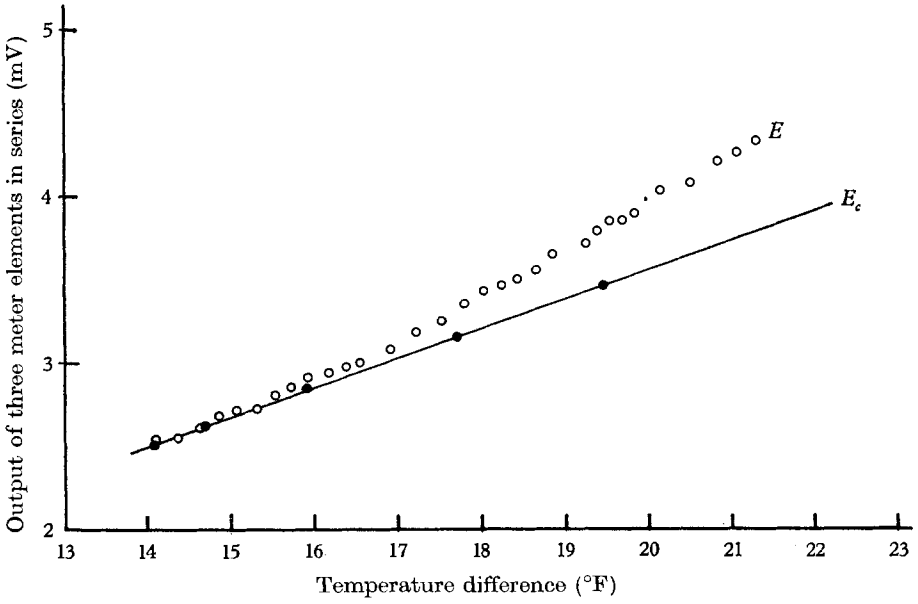

FIGURE 10. Variation of E and E_c with temperature difference.

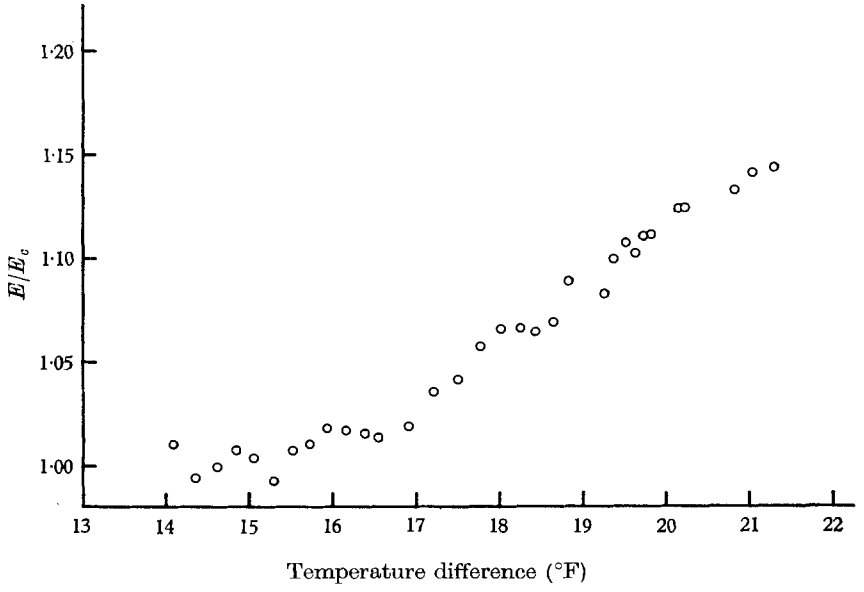

FIGURE 11. Effect of temperature difference on heat transfer across a horizontal layer of air 0·749 in. thick.

transition. The result obtained for R_{cr} by this method could not be distinguished from the one found by increasing pressure at a very slow rate, and it was concluded that the two processes for inducing transition are essentially equivalent. Moreover, at the low rates of change both processes could be regarded practically quasi-steady.

As a further check on the apparatus, the outputs of the individual heat flow meters in the bottom plate were monitored on a multipoint Leeds & Northrup potentiometer recorder. The records indicated the onset of convection at all the locations practically simultaneously. Any one of the meters could have been employed to determine the critical Rayleigh number.

No dependence of the critical Rayleigh number on layer height was observed during the course of the experiments. This is significant in regard to the Biot number (hL/k) of the bounding surfaces† and to the columnar convection reported by Chandra and analysed by Sutton.

The work of Sparrow *et al.* shows that as the Biot number of the bounding surfaces decreases the critical Rayleigh number decreases. For the layer heights and gases investigated the Biot number changes by a factor of 12. From these results of Sparrow *et al.*, we conclude that the independence of the Biot and the critical Rayleigh numbers confirms that in our apparatus the surface temperatures are fixed.

Chandra reported columnar convection occurring at small layer heights and Sutton ascribed this phenomenon to the transient nature of Chandra's experiments. Our investigations at $\frac{1}{8}$ in. were in the range of layer height in which columnar convection had been observed. Since we found the critical Rayleigh number to be the same for the smallest gap as for the larger ones and the heat flow meter output remained independent of pressure below transition, we conclude that columnar convection did not occur in our experiments. Apparently our experiments were free from the rapid transients that had given rise to columnar convection, as explained by Sutton.

Regarding figure 12, one should imagine a set of 18 experimental curves spread out in the convective region. They represent 18 runs on the 0·749 in. air layer only, each run consisting of at least 10 observations of E/E_c and R. The ranges of the variables are as follows:

$$\Delta T = 11{\cdot}0 \quad \text{and} \quad 17{\cdot}5\,^{\circ}\text{F},$$

$$p = 450 \quad \text{to} \quad 740\,\text{mmHg},$$

$$T_a = 110 \quad \text{to} \quad 140\,^{\circ}\text{F}.$$

The average rate of pressure rise was about 1 mmHg/min. A reduction of the data was obtained by computing the mean values of E/E_c at the several values of R. These are represented by the points. A critical value $R_{cr} = 1793$ was established by extrapolating the line faired through those points until it intersected the line $E/E_c = 1{\cdot}0$. Bands of probable error in the ratio E/E_c are shown at the values of R where the ratio was computed. Limits of the probable error in the value of the critical Rayleigh number were established by constructing curves

† h denotes the unit surface conductance exterior to the fluid layer.

through the extremes of the individual bands of probable error in E/E_c. Thus it was established that $R_{cr} = 1793 \pm 18$, which was also in agreement with the steady-state values.

These statistics show that this approach to the problem of determining critical Rayleigh numbers in gases yields substantially better repeatability than those employed in the past. Also, the resolution is good, since the total change of

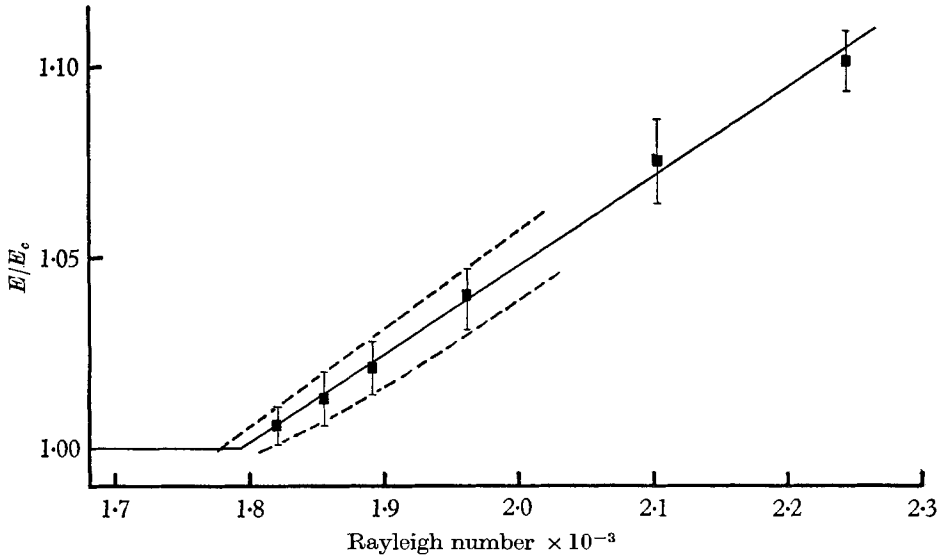

FIGURE 12. Variation of E/E_c with Rayleigh number.

R is small compared with changes that others have had to employ. (For example, compare Chandrasekhar's figure 14 in the same range of R as in the present experiments.) The results also indicate that the transition is extraordinarily well behaved. Our attempts to induce premature transition failed. Transition occurred beyond $R_{cr} = 1793$ only when the pressure was raised very rapidly. This is in contrast to the transition from laminar to turbulent flow in pipes, where the critical Reynolds number varies with small changes in the apparatus.

The substitution of continuous control in place of the on–off control on the top surface temperature and use of the bucking voltage and amplification to determine the onset of motion will reduce the mean random error. The present repeatability suggests that the apparatus may be used not only to determine transition but also to study the transport properties of gases and of mixtures of gases. Thus, the thermal conductivity could be determined from the heat flow meter output before transition and, with the critical value of the Rayleigh number established, the absolute viscosity could then be found from the transition conditions. Where either conductivity or viscosity is known, the other could be found from the transition point alone, measurements of absolute heat flux being unnecessary.

Average values of the critical Rayleigh number for the three gases investigated are presented in the following tabulation. None is as low as the theoretical value, 1708. However, this value lies at the extreme lower limit of the experi-

mental accuracy. The accuracy can be improved by instrumenting the cover plates so that their temperature difference ΔT can be measured with improved certainty, without interfering with the ΔT control.

Height of layer (in.)	Gas		
	Argon	Air	Carbon dioxide
$\frac{1}{8}$	1807	1804	—
$\frac{1}{4}$	1800	1775	1780
$\frac{3}{4}$	—	1793	—

5. Conclusions

1. Experiments have been performed on the Rayleigh–Jeffreys instability in argon, air and carbon dioxide layers $\frac{1}{8}$, $\frac{1}{4}$ and $\frac{3}{4}$ in. in height. Pressure ranged from about 0·6 to 6 atm. The experiments employed not only the traditional method in which the Rayleigh number is varied through the temperature difference, but also a new method in which the pressure is increased at a very slow rate while the temperature and temperature difference are held constant.

2. At the lowest rates of pressure rise, less than 2 mmHg/min, a single value of the Rayleigh number was found at the outset of convection, practically the same as the value found under steady-state conditions. The transition value was observed to be independent of the gap size, fluid, mean temperature, temperature difference, pressure, method of inducing the transition and severe mechanical disturbances.

3. The value of the critical Rayleigh number thus found was 1793, repeatable with a mean error of 1·0 %. On an absolute basis, considering errors from all sources except property values, we place our determination at 1793 ± 80. This is in reasonable agreement with the theoretical value, 1708, but the difference is probably significant of an unknown cause.

4. The subcritical columnar convection observed by Chandra in very thin layers was not observed in the $\frac{1}{8}$ and $\frac{1}{4}$ in. employed in the present investigation, apparently because the disturbances were applied relatively slowly.

5. When the pressure was increased at rates well above 2 mmHg/min, an increase was observed in the value of the critical Rayleigh number which could not be explained solely by the transient delay in the instrumentation, and it appears that rapid rates of pressure rise inhibit the development of convective motion.

6. This new experimental approach to the instability problem appears to be a highly promising technique for the measurement of the transport properties of gases. An *in situ* calibration of the heat flow meters, which is currently under way, will allow measurement of k. The pressure at which transition occurs will provide a measure of the product μk. Thus values of transport properties can be determined in a single apparatus.

Even at moderate temperature and pressure levels, few data are available on the transport properties of mixtures of gases. We believe the present technique has much to offer in investigations of the behaviour of ideal and non-ideal

gases. Another area where transport property data are almost non-existent is the region of very high temperature and very high pressure. The location of these two variables in equation (1.2) for the Rayleigh number shows that critical values may occur when both temperature and pressure are high. Although the equipment must clearly be redesigned for such an application the use of the technique appears to be limited only by the materials of construction and the availability of thermodynamic property values.

The authors gratefully acknowledge the support of the National Science Foundation under Grant 21392.

Appendix A

Delay of the heat flow meter response

Owing to the heat capacity of the copper cover plates, the meter output and the heat flux through the gas layer may not be in one-to-one correspondence during all tests. The following analysis, based on lumped parameters and proportional feedback control, provides an estimate of the time delay in the heat flow meter response to the onset of motion in the air layer.

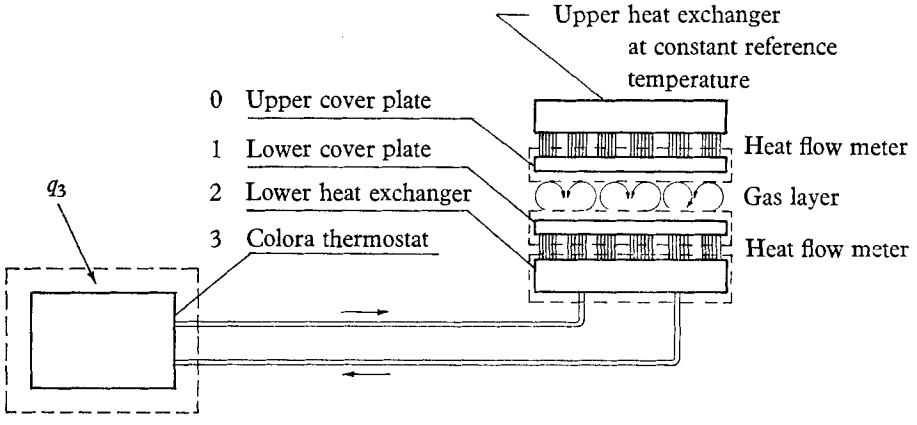

FIGURE 13. Schematic model for analysis of instrumentation response.

The entire system, shown schematically in figure 13, is divided into four subsystems indicated by the dotted control surfaces and numbered† $i = 0, 1, 2$ and 3. The mean temperature T_i of each subsystem is referred to the upper heat exchanger and the thermal capacities are W_i. The heat capacities of the gas layer and the mica wafers are negligible. Applying the first law to each subsystem we obtain the following system of equations in four degrees of freedom

$$W_0(dT_0/dt) + [C + C_0(t)]\,T_0 - C_0(t)\,T_1 = 0, \tag{A 1}$$

$$W_1(dT_1/dt) + [C' + C_0(t)]\,T_1 - C_0(t)\,T_0 - C'T_2 = 0, \tag{A 2}$$

$$W_2(dT_2/dt) + (C' + w)\,T_2 - CT_1 - wT_3 = 0, \tag{A 3}$$

$$W_3(dT_3/dt) + wT_3 - wT_2 = q_3. \tag{A 4}$$

† Subscripts 0 and 1 are now used where u and o were used in the main text.

The coefficients C, $C_0(t)$, and C' are the thermal conductances of the upper heat flow meter package, the gas layer, and the lower heat flow meter package, respectively; w denotes the water equivalent flow circulated by the lower thermostat. The heat input q_3 to the lower heat exchanger is controlled mainly proportionally according to the feedback relationship

$$q_3 = q_{3s} + K[(T_{1s} - T_{0s}) - (T_1 - T_0)], \tag{A 5}$$

K being the controller constant and subscript s signifying steady-state conditions.

The steady heat conduction through the gas layer is

$$q_{as} = C_{0s}(T_{1s} - T_{0s}). \tag{A 6}$$

For the unsteady heat transfer, which occurs when $p \geqslant p_{cr}$, it is convenient to introduce a new function $\eta(t)$, representing the excess heat transfer due to convection

$$C_0(t) = C_{0s} + \eta(t)/(T_{1s} - T_{0s}). \tag{A 7}$$

Further, we introduce the excess temperatures

$$\theta_i = T_i - T_{is}. \tag{A 8}$$

Upon elimination of q_3 from (A 4) and (A 5) and substitution from (A 7) and (A 8), the heat-balance equations become

$$W_0 d\theta_0/dt + (C + C_{0s})\,\theta_0 - C_{0s}\theta_1 = \eta(t), \tag{A 9}$$

$$W_1 d\theta_1/dt + (C' + C_{0s})\,\theta_1 - C'\theta_2 - C_{0s}\theta_0 = -\eta(t), \tag{A 10}$$

$$W_2 d\theta_2/dt + (C' + w)\,\theta_2 - C'\theta_1 - w\theta_3 = 0, \tag{A 11}$$

$$W_3 d\theta_3/dt + w\theta_3 - w\theta_2 + K\theta_1 - K\theta_0 = 0. \tag{A 12}$$

This set is to be solved under the initial conditions

$$\theta_i(0) = 0. \tag{A 13}$$

The forcing function η depends upon the Nusselt number Nu

$$\eta = (Nu - 1)\,C_{0s}(T_{1s} - T_{0s}). \tag{A 14}$$

Our measurements suggest that the Nusselt and Rayleigh numbers are linearly related and the following approximate relation has been developed solely for use in estimating the transient delay

$$Nu = 1 + 0{\cdot}42(R/R_{cr} - 1). \tag{A 15}$$

This equation is a tentative correlation of heat-transfer rates beyond the transition point; additional investigations of this subject are under way in our laboratory.

Observing that R is proportional to the square of the absolute pressure and assuming that the pressure increases at a constant rate m, we find that (A 14) and (A 15) yield

$$\eta(t) = 0{\cdot}42[(1 + mt)^2 - 1]\,C_{0s}(T_{1s} - T_{0s}), \tag{A 16}$$

where

$$m = \frac{1}{p_{cr}}\frac{dp}{dt} \approx \frac{p/p_{cr} - 1}{\Delta t}. \tag{A 17}$$

If $mt \ll 2$, a condition well satisfied during the first 10 min after the critical point, the second-order term in the time may be neglected. Introducing the constant

$$B = 0{\cdot}42C_{0s}(T_{1s} - T_{0s})/W_1, \tag{A 18}$$

we obtain, to a good approximation,

$$\eta(t) = 2W_1 Bmt. \tag{A 19}$$

The apparatus constants are approximately as follows:

$$W_0 = W_1 = 0{\cdot}28, \quad W_2 = 3{\cdot}0, \quad \text{and} \quad W_3 = 42\,\text{B.Th.U./°F}; \quad C = C' = 0{\cdot}17,$$
$$w = 12{\cdot}5, \quad \text{and} \quad K = 17\,\text{B.Th.U./min °F}.$$

The coefficient $C_{0s} \lesssim 0{\cdot}01$ B.Th.U/min °F. This relatively small value suggests that terms containing C_{0s} in (A 9) through (A 12) may be deleted. This omits the effects of deviations from the set temperature difference on the heat transferred through the layer; however, their effect on the controller is retained. The omission also simplifies the calculations because now (A 9) is coupled only unilaterally.

We introduce a new set of coefficients defined by the array

$$(\alpha_{ij}) = \begin{pmatrix} \frac{C}{W_1} & 0 & 0 \\ \frac{C}{W_2} & \frac{C+w}{W_2} & \frac{w}{W_2} \\ \frac{K}{W_3} & 0 & \frac{w}{W_3} \end{pmatrix} = \begin{pmatrix} 0{\cdot}6071 & 0{\cdot}0000 & 0{\cdot}0000 \\ 0{\cdot}0567 & 4{\cdot}2233 & 4{\cdot}1666 \\ 0{\cdot}4048 & 0{\cdot}0000 & 0{\cdot}2976 \end{pmatrix} \tag{A 20}$$

and a new set of dependent variables defined by

$$\Theta_i = \theta_i/2Bm. \tag{A 21}$$

Under the above simplifications and transformations, the governing equations become

$$d\Theta_0/dt + \alpha_{11}\Theta_0 = t, \tag{A 22}$$
$$d\Theta_1/dt + \alpha_{11}\Theta_1 - \alpha_{11}\Theta_2 = -t \tag{A 23}$$
$$d\Theta_2/dt + \alpha_{22}\Theta_2 - \alpha_{21}\Theta_1 - \alpha_{23}\Theta_3 = 0, \tag{A 24}$$
$$d\Theta_3/dt + \alpha_{33}\Theta_3 + \alpha_{31}\Theta_1 - \alpha_{33}\Theta_2 = \alpha_{31}\Theta_0, \tag{A 25}$$

and these are to be solved under (A 13).

The pertinent results are

$$\Theta_0 = 1{\cdot}647[t - 1{\cdot}647(1 - e^{-0{\cdot}607t})] \tag{A 26}$$

and

$$\Theta_2 - \Theta_1 = 2{\cdot}669 + 1{\cdot}647t - 2{\cdot}71\,e^{-0{\cdot}607t} + 0{\cdot}0106\,e^{-4{\cdot}58t} + e^{-0{\cdot}274t}[0{\cdot}0307\cos 0{\cdot}384t - 8{\cdot}421\sin 0{\cdot}384t]. \tag{A 27}$$

Results of the calculations are shown in figure 14 in which $C(\Theta_2 - \Theta_1)$, the response of the lower meter, is plotted against the time t in minutes. This is com-

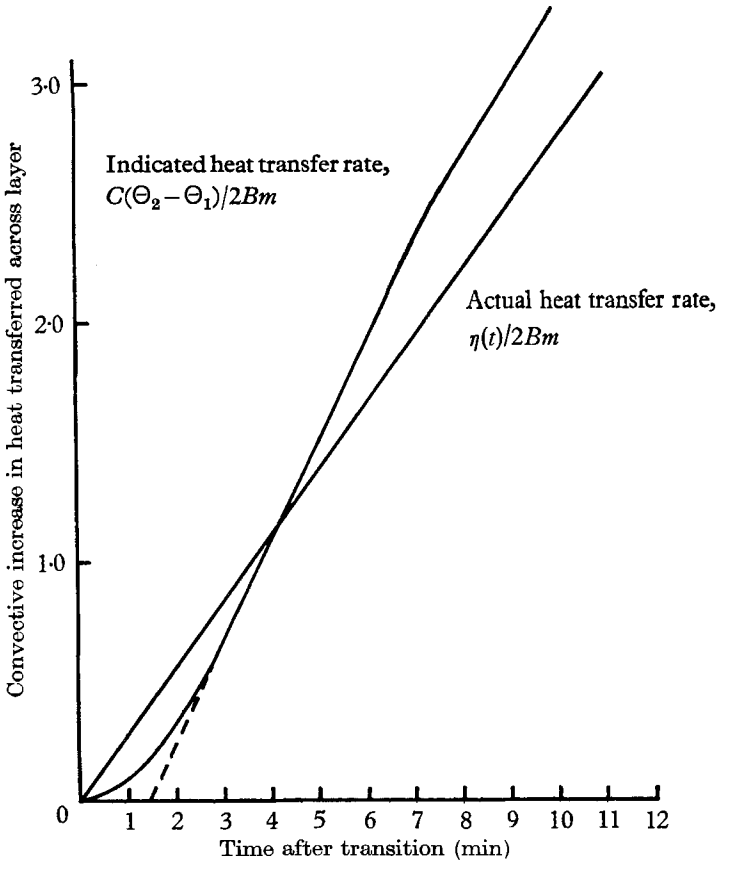

FIGURE 14. Transient response to the onset of convection.

pared to the heat flow through the gas layer, which is proportional to $W_1 t$. Clearly, there is a delay of about 1·5 min, after which the meter responds rather sharply.

Comparisons of experimental and analytical results were made for a $\frac{3}{4}$ in. air layer with $\Delta T = 18\,°\mathrm{F}$. Ten minutes after transition, θ_0 was measured to be $0{\cdot}1\,\mu\mathrm{V}$ as compared to $0{\cdot}14\,\mu\mathrm{V}$ from (A 26). Three lower meters in series gave $dE/dt = 12{\cdot}5\,\mu\mathrm{V/min}$ compared to $6{\cdot}6\,\mu\mathrm{V/min}$ calculated by means of (A 27). The agreement between these results is considered satisfactory in view of the simplifications of the model.

Appendix B

The dilatation and the specific heat

Early analyses of the instability problem modelled a fluid which was clearly a liquid. In such a case there was no practical reason to distinguish between the specific heats at constant pressure and at constant volume. Chandrasekhar, attempting to formalize the development of the theory for both liquids and gases, began his arguments with c_v, the specific heat at constant volume. Through an error in the development, the influence of the dilatation was lost. Consequently, the specific heat at constant volume appears in his definition of the

Rayleigh number instead of the specific heat at constant pressure. We append the following discussion in an attempt to show where the error lies, hoping that its propagation might cease.

Cartesian tensor notation is employed in a co-ordinate system $Ox_i (i = 1, 2, 3)$; where x_3 is vertical, positive sense upward. The velocity components are u_i and the dissipation function Φ. The specific heats, the dynamic viscosity, and the thermal conductivity are assumed constant. We omit the equations of motion (Chandrasekhar's equation (18)) and begin with the energy equation, because here the specific heat enters the analysis.

Under the above assumptions regarding the nature of the fluid the energy equation may be written exactly either in the form

$$\rho c_v \left(\frac{\partial T}{\partial t} + u_j \frac{\partial T}{\partial x_j}\right) = k\nabla^2 T - T\left(\frac{\partial p}{\partial T}\right)_\rho \frac{\partial u_m}{\partial x_m} + \Phi, \tag{B 1a}$$

or in the *completely equivalent* form (Bird, Stewart & Lightfoot 1960),

$$\rho c_p \left(\frac{\partial T}{\partial t} + u_j \frac{\partial T}{\partial x_j}\right) = k\nabla^2 T - \left(\frac{\partial \ln \rho}{\partial \ln T}\right)_p \cdot \left(\frac{\partial p}{\partial t} + u_j \frac{\partial p}{\partial x_j}\right) + \Phi. \tag{B 1b}$$

The continuity equation is

$$\frac{\partial \rho}{\partial t} + u_j \frac{\partial \rho}{\partial x_j} = -\rho \frac{\partial u_m}{\partial x_m}. \tag{B 2}$$

Under the assumption of a thermally perfect gas, equation (1.3), the differential coefficients are $T(\partial\rho/\partial T)_\rho = p$ and $(\partial \ln \rho/\partial \ln T)_p = -1$. Substitution of the first of these into (B 1*a*) yields the energy equation in the form used by Chandrasekhar,

$$\rho c_v \left(\frac{\partial T}{\partial t} + u_j \frac{\partial T}{\partial x_j}\right) = k\nabla^2 T - p \frac{\partial u_m}{\partial x_m} + \Phi. \tag{B 3a}$$

The equivalent form employing the specific heat at constant pressure is

$$\rho c_p \left(\frac{\partial T}{\partial t} + u_j \frac{\partial T}{\partial x_j}\right) = k\nabla^2 T + \frac{\partial p}{\partial t} + u_j \frac{\partial p}{\partial x_j} + \Phi. \tag{B 3b}$$

The pure conduction or unperturbed solution is now signified by barred symbols. The energy and continuity equations and the boundary conditions are satisfied by

$$\bar{u}_i = 0 \quad \text{and} \quad \bar{T} = T_0 - \beta x_3, \tag{B 4}$$

the constant β being defined so that $\bar{T}$ takes the value of the fixed temperature prescribed at $x_3 = L$.

The momentum equations in the x_1 and x_2 directions simply assure us that $\bar{p}$ is a function only of x_3, and the equation for the third component of momentum reduces to the condition of hydrostatic equilibrium; $d\bar{p}/dx_3 = -g\bar{\rho}$. By employing this equation together with (1.3) and (B 4) the distributions of $\bar{p}$ and $\bar{\rho}$ are found to be

$$\bar{p} = p_0 (1 - \beta x_3/T_0)^{g/\beta\mathscr{R}}, \quad \bar{\rho} = \rho_0 (1 - \beta x_3/T_0)^{(g/\beta\mathscr{R})-1}. \tag{B 5}$$

In our experiments $\beta \approx 240\,°\text{F/ft.}$ and $T_0 \approx 576\,°\text{R}$; therefore the exponent $g/\beta\mathscr{R} \approx 10^{-4}$, and the right-hand members of (B 5) are adequately represented

by the first two terms of their expansions: $\overline{p} = p_0 - \rho_0 g x_3$ and $\overline{\rho} = \rho_0(1 + \alpha_0 \beta x_3)$. These are the results obtained when the fluid is assumed incompressible at the outset, that is when (1.3) is replaced by $\rho = \rho_0[1 - \alpha_0(T - T_0)]$, as has always been done for a liquid.

Perturbations on $\overline{u}_i$, $\overline{T}$, $\overline{p}$ and $\overline{\rho}$ are denoted by u_i, θ, $\tilde{p}$ and $\tilde{\rho}$, respectively. The last three are related by (1.3)

$$d\ln\rho = d\ln p - d\ln T \quad \text{or} \quad \tilde{\rho} \approx \rho_0(\tilde{p}/p_0 - \theta/T_0). \tag{B 6}$$

The linear perturbation of the continuity equation (B 2) is carried out in detail. The completely perturbed equation is

$$\underset{\text{(a)}}{\frac{\partial\overline{\rho}}{\partial t}} + \underset{\text{(b)}}{u_j\frac{\partial\overline{\rho}}{\partial x_j}} + \underset{\text{(c)}}{\frac{\partial\tilde{\rho}}{\partial t}} + \underset{\text{(d)}}{u_j\frac{\partial\tilde{\rho}}{\partial x_j}} = \underset{\text{(e)}}{-\overline{\rho}\frac{\partial u_m}{\partial x_m}} \underset{\text{(f)}}{-\tilde{\rho}\frac{\partial u_m}{\partial x_m}}. \tag{B 7}$$

The letters in parentheses are for reference. Term (a) is zero by definition. Terms (d) and (f) are of second (higher) order and are omitted. By virtue of (B 5), term (b) is $\rho_0\alpha_0\beta$. Hence, employing (B 6) and observing that $\overline{\rho} \approx \rho_0$ and $\alpha_0 \approx \alpha$, and that $\partial(\tilde{p}/p_0)/\partial t$ is also a product of two small quantities, we arrive at

$$\alpha\beta u_3 - \alpha(\partial\theta/\partial t) = -\partial u_m/\partial x_m. \tag{B 8}$$

This result is in complete agreement with that of Chandrasekhar. However, at this point in his argument he makes the sweeping statement that, since each of the terms on the left contains α, which is very small, the entire member is of second order compared to $\partial u_m/\partial x_m$. Thus he deduces the 'solenoidal character' of the velocity field and immediately employs this result to delete the reversible work from the energy equation (B 3*a*).

The argument fails to recognize that although the dilatation is small it is multiplied by a very large quantity, namely the absolute pressure, and the product is not a negligible contribution to the energy equation. As a consequence of this erroneous deletion, c_v permeates all the results. The proper accounting shows that the second term in (B 8) may be omitted, but not the first. Thus, in our experiments $\alpha \approx 0{\cdot}002\,^\circ\mathrm{F}^{-1}$ and $\beta \approx 240\,^\circ\mathrm{F/ft.}$, so that the term

$$\alpha\beta u_3 \approx 0{\cdot}5 u_3,$$

which is of the same order as the velocity perturbation. Accordingly, for a gas one must write

$$\partial u_m/\partial x_m = -\alpha\beta u_3, \quad \text{or} \quad \partial u_m/\partial(x_m/L) = -\Delta T u_3/T_a. \tag{B 9}$$

In words, an elemental fluid particle expands as it descends and contracts as it ascends. When liquids, particularly water or mercury, are employed in this experiment both α and β are about one order of magnitude smaller than they are in experiments with gases. It is then indeed reasonable that the dilatation be set equal to zero; the reversible work is practically zero and the specific heats are so nearly equal that no practical distinction can be made. In a gas this process is important to the energy transport and cannot be neglected, even though $\Delta T/T$ is only of the order 0·01.

The linear perturbation of (B 3*a*) yields

$$-\rho_0 c_v \beta u_3 + \rho_0 c_v (\partial\theta/\partial t) = k\nabla^2\theta - p_0(\partial u_m/\partial x_m). \tag{B 10}$$

Upon introduction of (B 9) and the facts that $\alpha_0 p_0 = R\rho_0$ and $c_v + R = c_p$, (B 10) becomes

$$\gamma^{-1}\partial\theta/\partial t = \kappa\nabla^2\theta + \beta u_3, \tag{B 11}$$

where $\gamma = c_p/c_v$. Similarly, the linear perturbation of (B 3*b*) yields

$$\partial\theta/\partial t - (\rho_0 c_p)^{-1}\,\partial\tilde{p}/\partial t = \kappa\nabla^2\theta + (\beta - g/c_p)\,u_3. \tag{B 12}$$

The left sides of (B 11) and (B 12) become zero when the principle of the exchange of stabilities is invoked. The term g/c_p is the one pointed out by Jeffreys (1930). Of the order 0·005 °F/ft., it is very small compared to β and consequently negligible. The implications of (B 3*a*) and (B 3*b*) are now seen to be equivalent, as had certainly to be expected, and they are consistent with the experimental findings, which show that, indeed, c_p must be used in the Rayleigh criterion.

Some possible ramifications of (B 9) warrant discussion. First, while the non-zero dilatation appears in the momentum equation, it is eliminated with $\tilde{\rho}$ (cf. $\delta\rho$, Chandrasekhar's equations (60), (64), and (67)), and the final result of the instability calculation is not affected by its presence. Secondly, the dilatation affects the boundary conditions in some cases. Here it becomes necessary to distinguish between rigid and free surfaces.

(*a*) *Rigid surface.* $u_1 = 0$, $u_2 = 0$, $u_3 = 0$. Further, since at the surface

$$\partial u_1/\partial x_1 = 0 \quad \text{and} \quad \partial u_2/\partial x_2 = 0,$$

it follows from (B 9) that $\partial u_3/\partial x_3 = 0$. Summarizing, $u_3 = 0$ and $\partial u_3/\partial x_3 = 0$, exactly as in the case that the dilatation is zero. Therefore, the theoretical critical Rayleigh number for the gas layer between two rigid surfaces is unchanged under (B 9).

(*b*) *Free surface.* $u_3 = 0$; and, since the shear stresses are zero,

$$\mu(\partial u_1/\partial x_3 + \partial u_3/\partial x_1) = 0 \quad \text{and} \quad \mu(\partial u_2/\partial x_3 + \partial u_3/\partial x_2) = 0. \tag{B 13}$$

Differentiating (B 9) with respect to x_3, interchanging the order of differentiation in the mixed derivatives and observing that by virtue of (B 13) both $\partial u_1/\partial x_3$ and $\partial u_2/\partial x_3$ are zero, we get

$$\partial^2 u_3/\partial x_3^2 + \alpha\beta\,\partial u_3/\partial x_3 = 0. \tag{B 14}$$

Summarizing, $u_3 = 0$ and (B 14) are to be satisfied at a free surface. The latter is in contrast to the condition $\partial^2 u_3/\partial x_3^2 = 0$ employed by Rayleigh (1916) and others. Thus we see that for a gas with a free surface the dimensionless parameter $\Delta T/T_a$ would play a role independently of its appearance in the Rayleigh number. There is no basic difficulty in achieving solutions for this case since the boundary conditions are still homogeneous. A few such solutions are needed to show the dependence of R_{cr} on $\Delta T/T_a$.

REFERENCES

BIRD, R. B., STEWART, W. E. & LIGHTFOOT, E. N. 1960 *Transport Phenomena* §10.4. New York: John Wiley.

CHANDRA, K. 1938 Instability of fluids heated from below. *Proc. Roy. Soc.* A, **164**, 231.

CHANDRASEKHAR, S. 1961 *Hydrodynamic and Hydromagnetic Instability*, Chapters I and II. Oxford University Press.

DE GRAAF, J. G. A. & VAN DER HELD, E. F. M. 1953 The relation between the heat transfer and the convection phenomena in enclosed plane air layers. *Appl. Sci. Res.* A, **3**, 393–409.

HILSENRATH, J., BECKETT, C., BENEDICT, W. S., FANO, L., HOGE, H. J., MASI, J. F., NUTALL, R. L., TOULOUKIAN, Y. S. & WOOLLEY, H. W. 1955 *Tables of Thermal Properties of Gases.* N.B.S. Circular 564.

JAKOB, M. 1957 *Heat Transfer*, volume II, pp. 13–33. New York: John Wiley.

JEFFREYS, H. 1930 The instability of a compressible fluid heated below. *Proc. Camb. Phil. Soc.* **26**, 170.

OSTRACH, S. 1957 Convection phenomena in fluids heated from below. *Trans. A.S.M.E.* **79**, 299.

PELLEW, A. & SOUTHWELL, R. 1940 *Proc. Roy. Soc.* A, **176**, 312.

RAYLEIGH, LORD 1916 On convection currents in a horizontal layer of fluid when the higher temperature is on the under side. *Phil. Mag.* **32**, 529.

SCHMIDT, E. & SILVERSTON, P. L. 1959 Natural convection in horizontal liquid layers. *Chem. Engr. Progr. Symposium Series 29*, **55**, 163.

SCHMIDT, R. J. & MILVERTON, S. W. 1935 On the instability of a fluid when heated from below. *Proc. Roy. Soc.* A, **152**, 586.

SCHMIDT, R. J. & SAUNDERS, O. A. 1938 On the motion of a fluid heated from below. *Proc. Roy. Soc.* A, **165**, 216.

SPARROW, E. M., GOLDSTEIN, R. J. & JONSSON, V. K. 1964 Thermal instability in a horizontal fluid layer: effect of boundary conditions and non-linear temperature profile. *J. Fluid Mech.* **18**, 513.

SUTTON, O. G. 1950 On the stability of a fluid heated from below. *Proc. Roy. Soc.* A, **204**, 297.

THOMPSON, H. A. 1964 A new and improved method for the determination of the critical Rayleigh number in gases. Ph.D. Thesis in Mechanical Engineering, Tulane University.